Constraint on the maximum mass of neutron stars using GW170817 event

Masaru Shibata,[1,2] Enping Zhou,[1] Kenta Kiuchi,[1,2] and Sho Fujibayashi[1]

[1]*Max Planck Institute for Gravitational Physics (Albert Einstein Institute),*
Am Muhlenberg 1, Potsdam-Golm 14476, Germany
[2]*Yukawa Institute for Theoretical Physics, Kyoto University, Kyoto, 606-8502, Japan*

We revisit the constraint on the maximum mass of cold spherical neutron stars coming from the observational results of GW170817. We develop a new framework for the analysis by employing both energy and angular momentum conservation laws as well as solid results of latest numerical-relativity simulations and of neutron stars in equilibrium. The new analysis shows that the maximum mass of cold spherical neutron stars can be only weakly constrained as $M_{\max} \lesssim 2.3\ M_\odot$. Our present result illustrates that the merger remnant neutron star at the onset of collapse to a black hole is not necessarily rapidly rotating and shows that we have to take into account the angular momentum conservation law to impose the constraint on the maximum mass of neutron stars.

I. INTRODUCTION

The first direct detection of gravitational waves from the coalescence of binary neutron stars (GW170817) [1] was accompanied with a wide variety of the observations of electromagnetic counterparts [2]. These observations give us new constraints for the properties of neutron stars. Gravitational-wave observation for the late inspiral phase of the binary neutron stars constrains the binary tidal deformability in the range of $100 \lesssim \Lambda \lesssim 800$ [3,4]. This suggests that the radius of the $1.4\ M_\odot$ neutron star would be in the range between $\sim$10.5 km and $\sim$13.5 km.

Electromagnetic observations, in particular a possible observation of a gamma-ray burst [5] and ultraviolet-optical-infrared observation [2,6], are also used for constraining the maximum mass of neutron stars. If we assume that the gamma-ray burst was driven from a remnant black hole surrounded by a torus, the black hole might have to be formed in a short timescale after the merger. In this hypothesis, Ref. [7] suggests that the maximum mass of neutron stars would be smaller than $2.16^{+0.17}_{-0.15}\ M_\odot$. Reference [8] suggests that the maximum mass of neutron stars would be 2.16–2.28 $M_\odot$, supposing that the merger remnant neutron star has the same mass as that of the inspiraling binary neutron star and is a rapidly rotating state (note that the actual mass of the remnant neutron star should be smaller: see Sec. II). The optical and infrared counterparts also suggest that the remnant massive neutron star would survive at least for several hundreds ms [9–12], while the absence of an extremely bright emission in the ultraviolet and optical bands at $\lesssim$1 d suggests that the remnant formed after the merger would collapse to a black hole within a timescale of $\sim$100 s after the merger [9,10,13]. This speculation could also give a constraint on the maximum mass of neutron stars, and Refs [9,10] suggest a fairly small value of the maximum mass as $\lesssim$2.2 $M_\odot$. However, these constraints are imposed in the assumption that the merger remnant neutron star is rapidly rotating at the onset of collapse; the constraint is imposed without taking into account details of the angular momentum dissipation process in the post-merger stage self-consistently.

In this paper, we revisit the constraint on the maximum mass of cold spherical neutron stars imposed by the observational results of GW170817. The analysis is done taking into account the evolution process in the postmerger phase of binary neutron stars, by carefully analyzing both energy and angular momentum conservation laws and by employing solid results of latest numerical-relativity simulations and of rotating neutron stars in equilibrium. In particular, we show that it is essential to take into account the angular momentum conservation for this kind of analysis. We then find that the maximum mass of cold spherical neutron stars could be as large as $\sim$2.3 $M_\odot$: that is, the upper bound may be by $\sim$0.1 $M_\odot$ larger than in our previous analysis [10]. We thus conclude that a simplified analysis and an inappropriate assumption lead to an inaccurate constraint on the maximum mass.

The paper is organized as follows. In Sec. II, we describe the assumptions imposed in our present analysis and the resulting basic equations. In Sec. III, we derive the constraint on the maximum mass of cold spherical neutron stars. Section IV is devoted to a summary. Throughout this paper, G and c denote the gravitational constant and speed of light, respectively.

II. ASSUMPTIONS AND BASIC EQUATIONS

In this paper, we postulate or assume the following interpretation for the observational results of neutron-star merger event GW170817. First, we postulate that a remnant neutron star was formed after the merger and survived temporarily as a quasisteady strong neutrino emitter. This is supported by the observations of electromagnetic (ultraviolet-optical-infrared) counterparts for the merger event [6], because the neutrino irradiation from the remnant neutron stars would play an important role for reducing the neutron richness and lanthanide fraction of the ejecta (e.g., Refs. [6,10–12]). Second, we postulate that the remnant neutron star collapsed to a black hole within the dissipation timescale of its kinetic energy via electromagnetic radiation like the magnetic dipole radiation (i.e., within ∼100 sec). This is because after the merger of binary neutron stars, magnetic fields are likely to be significantly amplified in the remnant neutron star [14] and in the presence of a strong energy injection comparable to the rest-mass energy of the ejecta by the electromagnetic radiation associated with large kinetic energy of the remnant, the ultraviolet-optical-infrared counterparts for GW170817 would be much brighter than the observational results [9,10]. However, it should be noted that if the angular momentum of the remnant neutron star is dissipated by gravitational radiation and/or carried away by mass ejection in a short timescale (e.g., ∼10 s), we may accept the formation of a stable neutron star, although this possibility is not very likely (see Sec. III D for a discussion). Third, we assume that the remnant neutron star at the onset of collapse was rigidly rotating. This could be a reasonable assumption for the case that the remnant neutron star was long-lived, because the degree of the differential rotation is likely to be reduced sufficiently via long-term angular momentum transport process (e.g., Ref. [15]). Thus, we suppose that the collapse of the remnant neutron star should occur at a turning point (a marginally stable state) along an equilibrium sequence of rigidly rotating supramassive neutron stars [16,17] (see Fig. 1 for turning points). Fourth, we postulate that an appreciable fraction of the baryon of mass ≳0.05 $M_\odot$ was located outside the black hole at its formation because the ultraviolet-optical-infrared observations for the GW170817 event indicate that the ejecta mass was likely to be ≳0.03 $M_\odot$ [6]. Finally, in this paper, we assume that neutron stars are described by simple nuclear matter equations of state (see the Appendix) and do not suppose other exotic possibilities like quark stars, twin stars, and hybrid stars (e.g., Ref. [18]). We also postulate that general relativity is a high-precision theory for neutron stars and binary neutron star mergers.

The quantities which are referred to in this paper are as follows: the baryon rest mass and gravitational mass at the formation of the binary neutron stars, M_* and M, respectively; the torus mass around the remnant neutron star and ejecta mass at the formation of a black hole, M_{out} and M_{eje},
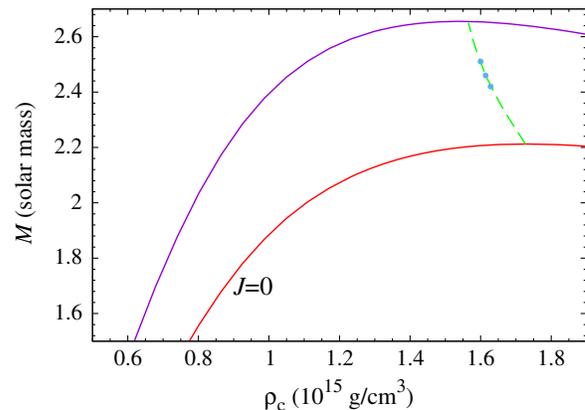

FIG. 1. Several important curves for rigidly rotating neutron stars in the plane of the gravitational mass (M) as a function of the central density (ρ_c). In this example, we employ EOS-6 (see Sec. III) as the neutron-star equation of state. The lower and upper solid curves show the sequences of nonrotating neutron stars (labeled by $J = 0$) and rigidly rotating neutron stars at mass shedding limits. The dashed curve shows the sequence of neutron stars that are marginally stable to gravitational collapse (the sequence of the turning points); the neutron stars in the lower-density side of this dashed curve are stable, otherwise they are unstable. The filled circles denote the predicted points at the onset of collapse for GW170817 in this model equation of state with $M_{out} + M_{eje} = 0.048$, 0.096, and 0.150 $M_\odot$ (from higher to lower mass: see Sec. III).

respectively; the total energy radiated by gravitational waves throughout the inspiral to postmerger phases, E_{GW}; total energy radiated by neutrinos throughout the merger to postmerger phases, E_ν; and the maximum mass for cold spherical neutron stars, M_{max}. Here, we know that $M = 2.74^{+0.04}_{-0.01}\, M_\odot$ with the 90% credible level [1,3]. In M_{out}, we include mass of an atmosphere surrounding the central object. E_{GW} can be divided into two parts: One is that emitted in the inspiral phase, $E_{GW,i}$, and the other is that in the merger and postmerger phases, $E_{GW,p}$. The subject of this paper is to constrain the value of M_{max} by using the relations satisfied among these quantities.

The first relation employed is the energy conservation law together with the rest-mass conservation law, which gives

$$M_{*f} := M_* - M_{out} - M_{eje} = f_{MS} M_f, \qquad (2.1)$$

where

$$M_f := M - E_{GW}c^{-2} - E_\nu c^{-2} - M_{out} - M_{eje}, \qquad (2.2)$$

and M_{*f} and M_f denote the rest mass and gravitational mass at the onset of collapse of the remnant neutron star, respectively. In Eq. (2.2), we assumed that the thermal, kinetic, and gravitational binding energy of the matter outside the remnant neutron star is much smaller than

(at most $\sim 10\%$ of) its rest-mass energy. This could affect the values of M_f, M_{out}, and M_{eje} only by $\sim 0.01 \, M_\odot$. We ignore the dissipation by electromagnetic radiation like the magnetic dipole radiation because in a short timescale of $\lesssim 10$ s which we consider here, the effect is likely to be negligible.

In Eq. (2.1), we denoted the ratio of the baryon rest mass to the gravitational mass for the remnant neutron star at the onset of collapse by $f_{\mathrm{MS}}(:= M_{*f}/M_f)$. For cold spherical neutron stars at a marginally stable state to collapse, the ratio of the baryon rest mass to the gravitational mass is $\approx 1.19 \pm 0.05$ (see Appendix). For rigidly rotating neutron stars near the marginally stable state, this value is smaller by a factor of up to ~ 0.02, and, thus, it depends only weakly on angular momentum (cf. Fig. 2 of Sec. III).

We also denote the ratio of M_* to M as $f_0 := M_*/M$. Since the ratio of the baryon rest mass to the gravitational mass is ~ 1.08–1.14 for realistic neutron stars with mass 1.2–$1.6 \, M_\odot$, f_0 should be $\approx 1.11 \pm 0.03$ (see Appendix).

For larger radii of neutron stars, f_0 and f_{MS} are in general smaller. It should be cautioned that the values of f_0 and f_{MS} depend on the equation of state and their deviation is not negligible for imposing the constraint to M_{max} within an error of $0.1 \, M_\odot$. Thus, in the analysis for constraining M_{max}, we must not use particular values for them.

By eliminating M_* from Eqs. (2.1) and (2.2), we finally obtain

$$M\left(1 - \frac{f_0}{f_{\mathrm{MS}}}\right)$$
$$= E_{\mathrm{GW}}c^{-2} + E_\nu c^{-2} + (M_{\mathrm{out}} + M_{\mathrm{eje}})\left(1 - \frac{1}{f_{\mathrm{MS}}}\right). \quad (2.3)$$

From Eqs. (2.2) and (2.3), we also obtain the gravitational mass at the onset of collapse as

$$M_f = \frac{f_0}{f_{\mathrm{MS}}}M - \frac{M_{\mathrm{out}} + M_{\mathrm{eje}}}{f_{\mathrm{MS}}}. \quad (2.4)$$

As we show in the Appendix, for cold spherical neutron stars of a variety of equations of state with the constraint that the tidal deformability of $1.35 \, M_\odot$ neutron stars, $\Lambda_{1.35}$, is smaller than 1000, the value of f_0/f_{MS} is approximately 0.920 ± 0.025. For this range, the left-hand side of Eq. (2.3) is found to be in a wide range as

$$M\left(1 - \frac{f_0}{f_{\mathrm{MS}}}\right) = 0.219^{+0.073}_{-0.069} \, M_\odot, \quad (2.5)$$

and also,

$$M_f = 2.521^{+0.106}_{-0.077} \, M_\odot - \frac{M_{\mathrm{out}} + M_{\mathrm{eje}}}{f_{\mathrm{MS}}}. \quad (2.6)$$

We note that f_{MS} depends only weakly on the angular momentum, as we find in Sec. III. Equations (2.5) and (2.6)

clearly illustrate that the dissipated energy and the gravitational mass at the onset of collapse have uncertain of approximately $\pm 0.1 \, M_\odot$ because the equation of state is not well constrained. As we show in the Appendix, the values of f_0/f_{MS} are correlated with M_{max}^{-1}. Thus, smaller values of M_{max} lead to larger values of M_f and to smaller energy dissipated from the system (see Sec. III).

The electromagnetic (ultraviolet-optical-infrared) counterpart observations for GW170817 show that the ejecta mass would be approximately $M_{\mathrm{eje}} \approx 0.03$–$0.05 \, M_\odot$ (e.g., Ref. [6]). This value is also supported by numerical simulations for a neutron star surrounded by a torus [15,19,20]. Numerical simulations (e.g., Refs. [10,15,21]) also indicate that the mass of the torus around the remnant neutron star would be ~ 0.1–$0.2 \, M_\odot$ for its early stage, and reduce to ~ 0.02–$0.05 \, M_\odot$ for its late stage $\tau \gtrsim 1$ s due to the mass ejection and mass accretion onto the remnant neutron star. Thus, M_{out} depends on the lifetime, τ, of the remnant neutron star. Also, at the formation of a black hole, it is decreased by $\gtrsim 50\%$ because a substantial fraction of the torus matter in the vicinity of the central object is swallowed by the black hole at its formation. Thus, we suppose $0.02 \, M_\odot \le M_{\mathrm{out}} \le 0.10 \, M_\odot$ at the collapse of the remnant neutron star in the following. For $M_{\mathrm{out}} = 0.06 \pm 0.04 \, M_\odot$, $(M_{\mathrm{out}} + M_{\mathrm{eje}})/f_{\mathrm{MS}}$ is approximately $(0.083 \pm 0.042)M_\odot$ and $(M_{\mathrm{out}} + M_{\mathrm{eje}})(1 - 1/f_{\mathrm{MS}})$ is $(0.016 \pm 0.008)M_\odot$, which is much smaller than the value of Eq. (2.5). Using this result, we approximately obtain

$$M_f = 2.44^{+0.15}_{-0.12} \, M_\odot, \quad (2.7)$$

and

$$(E_{\mathrm{GW}} + E_\nu)c^{-2}$$
$$= M\left(1 - \frac{f_0}{f_{\mathrm{MS}}}\right) - (M_{\mathrm{out}} + M_{\mathrm{eje}})\left(1 - \frac{1}{f_{\mathrm{MS}}}\right)$$
$$= (0.20 \pm 0.08) \, M_\odot. \quad (2.8)$$

Here, the large (small) side of the uncertainty in M_f comes basically from the large (small) values of f_0/f_{MS}, i.e., for small (large) values of $E_{\mathrm{GW}} + E_\nu$. Taking into account the uncertainty in these unknown values enlarges the uncertainty in the estimate of M_f compared with our previous estimation [10]. It should be also mentioned that the central value of M_f is by $\sim 0.15 \, M_\odot$ smaller than the value estimated in our previous paper [10]. The reason for this is that we underestimated the values of $E_{\mathrm{GW}} + E_\nu$ in the previous paper.

$(E_{\mathrm{GW}} + E_\nu)c^{-2}$ is found to be typically $\sim 0.2 \, M_\odot$ and at least larger than $\approx 0.12 \, M_\odot$. Numerical relativity simulations (e.g., Ref. [22]) have shown that $E_{\mathrm{GW,i}}$ is well constrained to be 0.035–$0.045 \, M_\odot c^2$ for $\Lambda_{1.35} \le 1000$. On the other hand, they show that $E_{\mathrm{GW,p}}$ depends strongly

on the equation of state. It could be $\sim 0.125\,M_\odot c^2 \approx 2.5 \times 10^{53}$ erg for the maximum case [22]. Note that $E_{\rm GW,p}$ should be smaller than the rotational kinetic energy of the remnant neutron star (see also Table II of Sec. III),

$$T = \frac{1}{2}I\Omega^2 \approx 2.3 \times 10^{53}\ {\rm erg}\left(\frac{M_{\rm MNS}}{2.6\,M_\odot}\right)\left(\frac{R_{\rm MNS}}{15\ {\rm km}}\right)^2$$
$$\times \left(\frac{\Omega}{10^4\ {\rm rad/s}}\right)^2, \tag{2.9}$$

where $M_{\rm MNS}$, $R_{\rm MNS}$, and Ω are the gravitational mass, equatorial circumferential radius, and angular velocity of the remnant neutron star, and we assumed that it is rigidly rotating (and hence its angular momentum is written as $2T/\Omega$). We note that the maximum angular velocity is approximately written as (see also Table II)

$$\Omega_K \approx \sqrt{GM_{\rm MNS}/R_{\rm MNS}^3}$$
$$\approx 1.01 \times 10^4\ {\rm rad/s}\left(\frac{M_{\rm MNS}}{2.6\,M_\odot}\right)^{1/2}\left(\frac{R_{\rm MNS}}{15\ {\rm km}}\right)^{-3/2}.$$
$$\tag{2.10}$$

As we find in the following, one of the key parameters for determining the angular momentum at the onset of collapse of the remnant neutron star is $E_{\rm GW,p}$. While $E_{\rm GW,p}$ could be $\sim 0.125\,M_\odot c^2$ if most of the rotational kinetic energy is dissipated by gravitational radiation, the post-merger evolution process is highly uncertain. If an efficient angular momentum transport works in the remnant neutron star and the degree of its nonaxisymmetric deformation is reduced quickly, $E_{\rm GW,p}$ would be of order $0.01\,M_\odot c^2$ [23]. These facts together with Eq. (2.5) suggest that an appreciable amount of energy of $\sim 0.1\,M_\odot c^2 \approx 2 \times 10^{53}$ erg would be dissipated by the emission of neutrinos until the onset of collapse to a black hole, unless the remnant neutron star radiates gravitational waves of energy comparable to T. Note that the value of $E_\nu \sim 10^{53}$ erg is quite natural if the remnant neutron star is long-lived with its lifetime $\tau \sim 1$ s because numerical-relativity simulations have shown that the neutrino luminosity from the remnant neutron star, L_ν, is of order 10^{53} erg/s (e.g., Refs. [24–26]). By contrast, if the remnant neutron star is relatively short-lived with $\tau \sim 100$ ms, E_ν would be of $O(10^{52}\ {\rm erg})$ (i.e., $\lesssim 0.01\,M_\odot c^2$), and, for this case, we have to employ a large value of $E_{\rm GW,p}$ to satisfy Eq. (2.8) (see Sec. III for more specific examples).

Since the remnant neutron star is rotating, the gravitational mass at the onset of collapse has to be larger than the maximum mass, $M_{\rm max}$, for cold spherical neutron stars by a factor of $f_r = M_f/M_{\rm max} > 1$. Here, the value of f_r is determined at a turning point along an equilibrium sequence of rigidly rotating neutron stars. If we could

obtain the value of f_r together with M_f, we can determine the value of $M_{\rm max}$. For the change of f_r by 0.1, $M_{\rm max}$ could be changed by $\approx 0.2\,M_\odot$. Thus, for constraining $M_{\rm max}$, e.g., within the $0.1\,M_\odot$ error, we have to determine the value of f_r within an error of ~ 0.05. For the maximally rotating neutron star along the turning point sequence, the value of f_r is known to be ~ 1.2 [17,27] (see also Fig. 2 of Sec. III) and this value has been often used for guessing the maximum mass of cold spherical neutron stars [7–10]. However, the remnant neutron star is not always rotating in such a high rotation speed as shown in Sec. III: In setting $f_r \approx 1.2$, one would assume a particular angular momentum of the remnant neutron star neglecting the angular momentum conservation. In addition, the maximum value of f_r depends on the equation of state (see Fig. 2 of Sec. III). It should be cautioned again that in the analysis for constraining the value of $M_{\rm max}$, we must not *a priori* employ a particular value for f_r.

For inferring the angular momentum of the remnant neutron star at the onset of collapse, we have to seriously analyze the dissipation of angular momentum in the postmerger phase. Let J_0 and J_f be the angular momentum at the onset of merger and at the onset of collapse of the remnant neutron star to a black hole, respectively. Then, we obtain

$$J_f = J_0 - J_{\rm GW,p} - J_\nu - J_{\rm out} - J_{\rm eje}, \tag{2.11}$$

where $J_{\rm GW,p}$, J_ν, $J_{\rm out}$, and $J_{\rm eje}$ are the angular momentum carried away (after the merger) by gravitational radiation, by neutrinos, angular momentum of the torus surrounding the remnant black hole at its formation, and angular momentum of ejecta (at the black-hole formation). In the following, we give or determine these quantities based on the results of numerical-relativity simulations. We also note that by angular momentum transport processes from the remnant neutron star to the surrounding matter, the angular momentum of torus and ejecta in general increases with time in the postmerger phase.

Since gravitational waves emitted in the postmerger phase are dominated by a fundamental mode of its frequency $f = 2$–4 kHz [28,29], $J_{\rm GW}$ is approximately written as

$$J_{\rm GW,p} \approx \frac{E_{\rm GW,p}}{\pi f}$$
$$\approx 9.5 \times 10^{48}\ {\rm erg\,s}\left(\frac{E_{\rm GW,p}}{0.05\,M_\odot c^2}\right)\left(\frac{f}{3.0\ {\rm kHz}}\right)^{-1}.$$
$$\tag{2.12}$$

Our latest numerical-relativity simulation confirms that this relation is satisfied within 1% accuracy [30]. Here, for the binaries of total mass $\approx 2.7\,M_\odot$, $f \approx 3.6$, 3.1, and 2.5 kHz for $R_{1.60} \approx 11$, 12, and 13.5 km [28,29], with R_M the radius

of a spherical neutron star of its gravitational mass M (in units of $M_\odot$). Thus, for $R_{1.35} \approx R_{1.60} \lesssim 13.5$ km (this constraint was given from the observational result of the tidal deformability of GW170817 [1,3]), $f \gtrsim 2.5$ kHz. In this paper, we infer the value of f by using the relation of Eq. (3) of Ref. [28].

Since the angular momentum of neutrinos is dissipated due to the fact that the emitter (remnant neutron star) is rotating, J_ν is written approximately by $J_\nu \approx (2/3)c^{-2}R_{MNS}^2\Omega E_\nu$ [31], and, thus,

$$J_\nu \approx 3.0 \times 10^{48} \text{ erg s} \left(\frac{E_\nu}{0.1 \ M_\odot c^2}\right)\left(\frac{R_{MNS}}{15 \text{ km}}\right)^2$$
$$\times \left(\frac{\Omega}{10^4 \text{ rad/s}}\right). \qquad (2.13)$$

We note that the value of J_ν described here agrees with the results of a numerical-relativity simulation within a factor of 2 [21]. Equation (2.13), in comparison with Eq. (2.12), illustrates that this is a non-negligible but minor effect for dissipating the angular momentum (thus, the error would be also a minor effect).

J_{out} is associated with the typical radius of the torus surrounding the remnant neutron star (at the onset of collapse). Denoting it by R_{out}, it is approximated by $J_{out} \approx M_{out}\sqrt{GM_{MNS}R_{out}}$, and, thus,

$$J_{out} \approx 5.8 \times 10^{48} \text{ erg s} \left(\frac{M_{out}}{0.05 \ M_\odot}\right)\left(\frac{R_{out}}{100 \text{ km}}\right)^{1/2}$$
$$\times \left(\frac{M_{MNS}}{2.6 \ M_\odot}\right)^{1/2}. \qquad (2.14)$$

Here R_{out} would be fairly small ~ 50 km in the early evolution stage of the accretion torus. However, during its long-term viscous evolution as well as angular momentum transport from the remnant neutron star, the typical radius increases to be $\gtrsim 100$ km for $\tau \gtrsim 300$ ms [15], which shows $R_{out} \approx 40 + 100(\tau/1 \text{ s})^{1/2}$ km for $\tau \lesssim 1.5$ s and, for a longer term, R_{out} approaches ~ 200 km.

J_{eje} is associated with the location at which the mass ejection occurs. Denoting the typical location by R_{eje}, it is approximated by $J_{eje} \approx M_{eje}\sqrt{GM_{MNS}R_{eje}}$, and, thus,

$$J_{eje} \approx 6.9 \times 10^{48} \text{ erg s} \left(\frac{M_{eje}}{0.05 \ M_\odot}\right)\left(\frac{R_{eje}}{140 \text{ km}}\right)^{1/2}$$
$$\times \left(\frac{M_{MNS}}{2.6 \ M_\odot}\right)^{1/2}. \qquad (2.15)$$

For long-lived remnant neutron stars which we consider in this paper, mass ejection mainly occurs through the long-term viscous process in the postmerger stage from an accretion torus [15,19,20] with mass $\sim 0.05 \ M_\odot$, while for dynamical mass ejection that occurs at merger, the matter

would be ejected at $R_{eje} \sim 30$ km with mass $\lesssim 0.01 \ M_\odot$. (Note that in M_{eje} both contributions are included.) Thus, for J_{eje}, only the postmerger mass ejection could contribute dominantly to the angular momentum loss. Since this mass ejection is driven from the torus, we simply set $R_{out} = R_{eje}$ in this paper; that is, we employ a relation as $J_{out} + J_{eje} = (M_{out} + M_{eje})\sqrt{GM_{MNS}R_{out}}$. Here, we may overestimate J_{eje} because the dynamical ejecta would have smaller angular momentum than the postmerger one. However, since the mass of the dynamical ejecta would be much smaller than the postmerger ejecta, the degree of the overestimation would be minor.

We note that the error for the estimate in $J_{out} + J_{eje}$ associated with the uncertainty in R_{out} would be of order 10%. This error will be reflected in $M_{out} + M_{eje}$ for determining it (see Sec. III). However, its error size does not affect our final conclusion.

Thus, besides J_0, the quantities in the right-hand side of Eq. (2.11) are related to E_{GW}, E_ν, M_{out}, and M_{eje} with f, Ω, M_{MNS}, and R_{out} as given parameters.

In addition, we have an important relation. From the definitions already shown, we obtain

$$f_r M_{max} = M_f = \frac{f_0}{f_{MS}}M - \frac{M_{out} + M_{eje}}{f_{MS}}. \qquad (2.16)$$

Thus, for a given value of f_r and $(M_{out} + M_{eje})/f_{MS}$, f_0/f_{MS} becomes a linear function of M_{max} as

$$\frac{f_0}{f_{MS}} = \frac{M_{out} + M_{eje}}{f_{MS}M} + \frac{f_r M_{max}}{M}. \qquad (2.17)$$

This becomes a condition that determines a particular state of the remnant neutron star at the onset of collapse for a given equation of state. This equation plays an important role in Sec. III.

Note that for larger values of M_f, $E_{GW,p} + E_\nu$ should be smaller, and, thus, the value of f_r should be larger because the collapse to a black hole should occur before a substantial fraction of angular momentum (and energy) is dissipated. Remembering the fact that M_f is correlated with M_{max}^{-1} for plausible equations of state (see Appendix), we then find that for the larger value of M_{max}, the required value of f_r is smaller. This fact clarifies that we cannot *a priori* give the value of f_r for constraining M_{max}.

III. ANALYSIS BASED ON NUMERICAL MODELING OF NEUTRON STARS AND BINARY NEUTRON STAR MERGERS

A. Preparation

In the analysis of Sec. II, we have several unknown parameters; f_0, f_{MS}, $E_{GW,i}$, $E_{GW,p}$, E_ν, f, Ω, M_{MNS}, M_{out}, M_{eje}, R_{MNS}, R_{out}, and J_0. Among them, f_0, f_{MS}, Ω, M_{MNS}, and R_{MNS} for a given equation of state are calculated (at
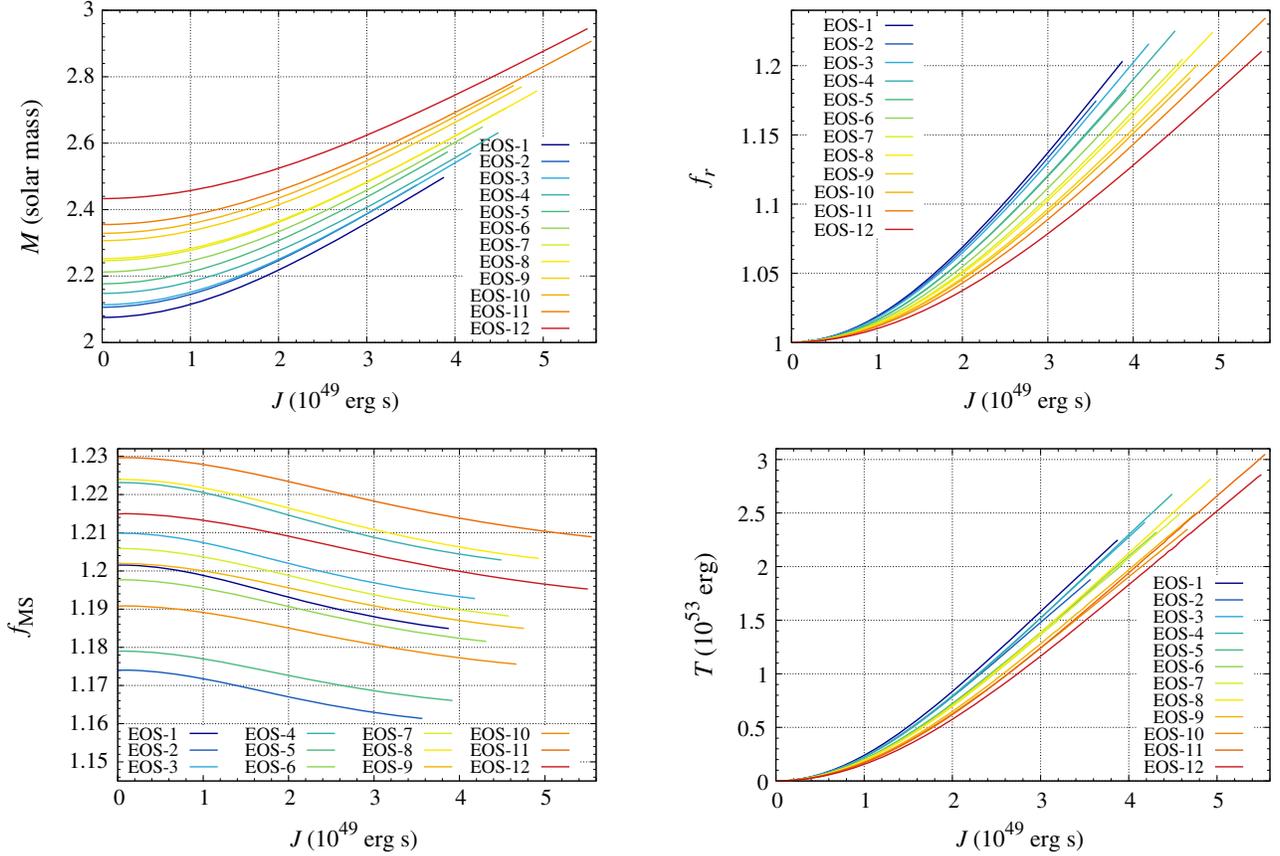
FIG. 2.   Gravitational mass, M, ratio of M to M_{max} (f_r), ratio of baryon rest mass to the gravitational mass, f_{MS}, and rotational kinetic energy $T = J\Omega/2$ as functions of J for rigidly rotating neutron stars along the marginally stable sequence (i.e., along the turning point sequence) with selected equations of state (see Table I). Note that M at $J = 0$ is M_{max}.

least with good approximation) by constructing equilibrium states of nonrotating and rotating neutron stars. Also, $E_{GW,i}$, f, M_{out}, M_{eje}, and R_{out} are approximately obtained with the help of numerical-relativity simulations, as already mentioned in Sec. II. J_0 is also obtained accurately with the help of numerical relativity. The dependence of J_0 on total binary mass m_0, symmetric mass ratio [hereafter referred to as $\eta(\leq 1/4)$], and $R_{1.35}$ is determined by the results by numerical relativity simulations [30] as

$$J_0 \approx Gc^{-1}m_0^2\eta[a_1 - a_2\delta\eta + a_3\bar{R}_{1.35}^3(1 + a_4\delta\eta)], \quad (3.1)$$

where $\bar{R}_{1.35}$ denotes $R_{1.35}$ in units of 10 km, $\delta\eta = \eta - 1/4(\leq 0)$, $a_1 \approx 3.32$, $a_2 \approx 31$, $a_3 \approx 0.137$, and $a_4 \approx 27$. We note that J_0 increases with the increase of $R_{1.35}$ and with the decrease of η because the merger occurs at a more distant orbit for larger stellar radii and for more asymmetric binaries.

Equation (3.1) shows that J_0 is in the range between $\approx 5.8 \times 10^{49}$ erg s and $\approx 6.3 \times 10^{49}$ erg s for neutron stars with $R_{1.35} = 10.5$–14 km, total mass $m_0 \approx 2.74 \, M_\odot$, and $\eta = 0.244$–0.250 (i.e., mass ratio 0.73–1.00). The value of J_0 is by $\sim 1 \times 10^{49}$ erg s larger than the maximum angular

momentum of rigidly rotating neutron stars (see Fig. 2) and $2T/\Omega$ for $\Omega \approx \Omega_K$ [see Eq. (2.9)], and this fact suggests that the remnant neutron star would initially have a differentially rotating state with the maximum angular velocity slightly larger than Ω_K, as has been found in many numerical-relativity simulations since Ref. [32].

In contrast to J_0 and $E_{GW,i}$, $E_{GW,p}$ and E_ν are not determined into a narrow range although $E_{GW,p} + E_\nu$ is constrained by Eq. (2.8) for given values of f_0/f_{MS}, $E_{GW,i}$, and $(M_{out} + M_{eje})/f_{MS}$ fairly well. We note that E_ν is associated with the lifetime of the remnant neutron star of GW170817, τ, as $E_\nu \approx L_\nu\tau$. Here, the neutrino luminosity is $L_\nu \gtrsim 10^{53}$ erg/s [21], but τ is not very clear. Thus, we consider $E_{GW,p}$ and E_ν as values to be determined in the present analysis.

In the following, we constrain the value of M_{max} by analyzing rigidly rotating neutron stars at marginally stable states (at turning points) for several equations of state. For computing rigidly rotating neutron stars in equilibrium, we employ a piecewise polytropic equation of state, for which the details are described in Appendix. The selected equations of state used in this section are listed in Table I. We selected many equations of state rather randomly for each

TABLE I.　Selected piecewise polytropic equations of state and important quantities for spherical neutron stars. The units of the mass and radius are $M_\odot$ and kilometer, and that of p is dyn/cm^2. f_{MS} is the ratio of the baryon rest mass to M_{max} for the maximum mass neutron star. f_0 shown here is M_*/M for binaries of mass 1.35 $M_\odot$ and 1.40 $M_\odot$. f denotes the dominant frequency of postmerger gravitational waves predicted approximately by the formula in Ref. [28].

Model	Γ_2	Γ_3	$\log_{10} p$	M_{max}	f_{MS}	$R_{1.60}$	$R_{1.35}$	$\Lambda_{1.35}$	f_0	f (kHz)
EOS-1	3.15	2.81	34.350	2.075	1.200	11.27	11.30	366.6	1.113	3.45
EOS-2	2.60	2.84	34.550	2.106	1.172	12.67	12.94	746.0	1.092	2.71
EOS-3	3.45	2.70	34.300	2.113	1.208	11.17	11.12	348.2	1.117	3.50
EOS-4	3.80	2.80	34.200	2.147	1.221	10.91	10.80	302.8	1.122	3.62
EOS-5	2.70	2.78	34.575	2.176	1.177	12.88	13.06	821.9	1.092	2.65
EOS-6	3.00	2.80	34.500	2.212	1.196	12.21	12.25	599.0	1.102	3.01
EOS-7	3.15	2.81	34.475	2.246	1.204	12.06	12.04	555.7	1.105	3.08
EOS-8	3.65	2.78	34.325	2.252	1.222	11.39	11.27	395.2	1.116	3.40
EOS-9	3.05	2.80	34.550	2.306	1.200	12.57	12.56	720.7	1.099	2.74
EOS-10	2.85	2.85	34.625	2.328	1.189	13.24	13.29	967.6	1.092	2.55
EOS-11	3.80	2.50	34.375	2.353	1.229	11.66	11.50	459.7	1.113	3.27
EOS-12	3.25	2.78	34.575	2.433	1.212	12.68	12.60	757.8	1.100	2.70

range of M_{max}. For the analysis, we only employ the equations of state with which 2 $M_\odot$ neutron stars [33] are reproduced, $\Lambda_{1.35} \leq 1000$, and the sound speed is always smaller than the speed of light for stable neutron stars. We ignore the thermal effect of the remnant neutron star for constructing equilibrium rotating neutron stars because it is a minor contribution to the neutron-star properties if we consider its age to be of order 0.1–1 s [34].

Figure 2 displays several key quantities as functions of the angular momentum, J, along the sequences of the marginally stable neutron stars (cf. the dashed curve of Fig. 1). Here, the neutron stars with $J = 0$ denote the marginally stable state for the spherical neutron stars of mass M_{max}, and at $J = J_{max}$, the neutron stars are at the mass-shedding limit; the angular velocity at the equatorial surface is equal to the Keplerian one. Table II also lists several quantities of a rigidly rotating neutron star at a turning point and mass shedding limit.

Figure 3 displays the relation between f_0/f_{MS} and M_{max} for marginally stable rigidly rotating neutron stars with several piecewise polytropic equations of state. Here, f_0 is calculated for binaries of mass $(1.35_\odot, 1.40 M_\odot)$ and $(1.20_\odot, 1.55 M_\odot)$, but the values for the two cases are different only by 0.2–0.3% (see the results in Appendix), and thus, the difference in f_0 is not very important in the following. The uncertainty in Fig. 3 reflects the variation of f_{MS} for the different angular momentum of the marginally stable rotating neutron stars: As found from Fig. 2, f_0/f_{MS} is smallest for $J = 0$ and largest for $J = J_{max}$. The tilted lines in Fig. 3 show the relation of Eq. (2.17) for $f_r = 1.20 - 0.02 \times i$ up to 1.00 (from left to right) with $(M_{out} + M_{eje})/f_{MS} = 0.04\ M_\odot$ and $0.08\ M_\odot$, while M is fixed to be 2.74 $M_\odot$. We note that for a given value of M_{max}, the value of f_0/f_{MS} is in general larger for the larger values of $\Lambda_{1.35}$, and, hence, the upper bound is determined by the constraint for $\Lambda_{1.35}$ (see Appendix).

TABLE II.　Key quantities for rigidly rotating neutron stars at the maximum mass along the marginally stable sequences for selected equations of state listed in Table I. $M_{MS,R}$: gravitational mass, $M_{*MS,R}$: baryon rest mass, $J_{MS,R}$: angular momentum, $\Omega_{MS,R}$: angular velocity, $T_{MS,R}$: rotational kinetic energy, and $R_{MS,R}$: circumferential radius at the equatorial surface.

| Model	$M_{MS,R}$ ($M_\odot$)	$M_{*MS,R}/M_{MS,R}$	$M_{MS,R}/M_{max}$	$J_{MS,R}$ (10^{49} erg s)	$\Omega_{MS,R}$ (10^4 rad/s)	$T_{MS,R}$ (10^{53} erg)	$R_{MS,R}$ (km)
EOS-1	2.497	1.185	1.203	3.875	1.160	2.247	13.04
EOS-2	2.474	1.161	1.175	3.567	1.055	1.880	13.74
EOS-3	2.570	1.193	1.216	4.183	1.155	2.415	13.15
EOS-4	2.631	1.203	1.225	4.492	1.192	2.677	13.11
EOS-5	2.574	1.167	1.183	3.919	1.028	2.014	14.19
EOS-6	2.649	1.182	1.198	4.315	1.077	2.323	13.87
EOS-7	2.707	1.188	1.205	4.580	1.090	2.496	13.93
EOS-8	2.757	1.203	1.224	4.932	1.143	2.819	13.73
EOS-9	2.770	1.185	1.208	4.756	1.049	2.494	14.33
EOS-10	2.774	1.176	1.191	4.668	1.007	2.349	14.79
EOS-11	2.907	1.209	1.234	5.548	1.099	3.049	14.26
EOS-12	2.945	1.195	1.210	5.504	1.039	2.858	14.77
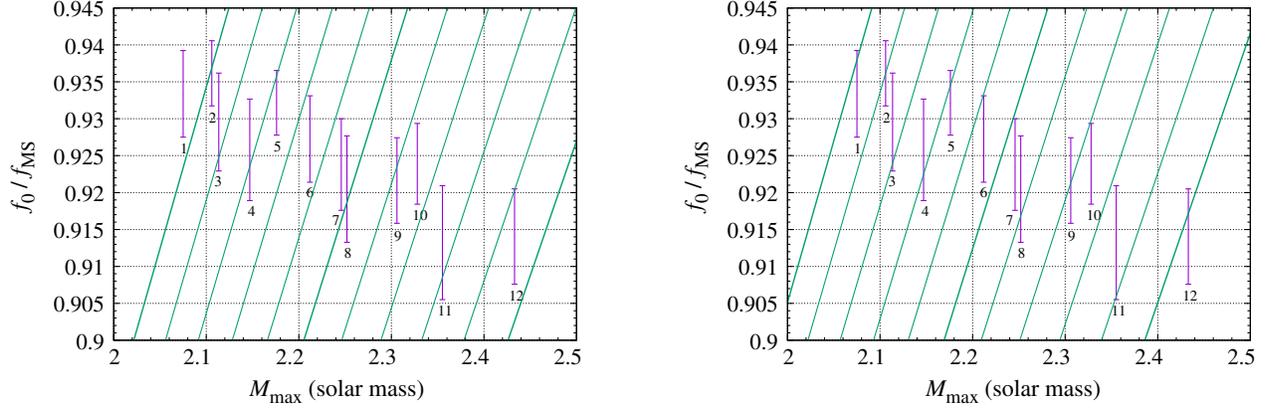
FIG. 3.   Relation between f_0/f_{MS} and M_{max} for marginally stable rigidly rotating neutron stars with several equations of state listed in Table I. The lower and upper ends of each uncertainty range correspond to $J = 0$ and $J = J_{max}$, respectively. The numbers attached in each data denote the model equations of state. The tilted lines show the relation of Eq. (2.17) for $f_r = 1.20, 1.18, 1.16, …, 1.04, 1.02,$ and 1.00 (from left to right) with $(M_{out} + M_{eje})/f_{MS} = 0.04\ M_\odot$ (left panel) and $0.08\ M_\odot$ (right panel) and with $M = 2.74\ M_\odot$. The thick lines are for $f_r = 1.20, 1.10,$ and 1.00.

For rigidly rotating neutron stars, the upper limit of f_r is approximately 1.2 as found from Fig. 2 (see also Table II). Thus, the left region of the line of $f_r = 1.2$ in Fig. 3 is prohibited in our model. That is, for the equations of state with small values of $M_{max} = 2.0$–$2.1\ M_\odot$, the remnant neutron star cannot achieve the rigidly rotating state at the onset of collapse (we show the examples in Sec. III C). For such equations of state, the remnant neutron star would collapse before the rigidly rotating state is achieved; i.e., its lifetime is shorter than the angular momentum transport timescale in the remnant neutron star. It is natural to consider that the lifetime of the remnant neutron star with such equations of state is fairly short $\ll 1$ s.

For the right region of the line of $f_r = 1$, on the other hand, the collapse cannot occur, because the mass of the remnant neutron star is smaller than M_{max}. Thus, for such equations of state, a stable neutron star should be the final outcome. As mentioned in the first paragraph of Sec. II, if such a stable remnant is formed in GW170817 and has large rotational kinetic energy $\gtrsim 10^{52}$ erg, an energy injection to ejecta through electromagnetic radiation like the magnetic dipole radiation would occur and be inconsistent with the observational results for the electromagnetic counterparts of GW170817 [9,10]. However, if the rotational kinetic energy is dissipated or removed in a short timescale ($\lesssim 100$ s), e.g., by gravitational radiation and neutrino emission, we may accept the formation of a stable neutron star [35].

Figure 3 shows an important fact as follows: If the maximum mass of spherical neutron stars in nature is relatively small $\lesssim 2.1\ M_\odot$, the collapse would occur for the remnant neutron star in a rapidly rotating state with $f_r \approx 1.2$. On the other hand, if the maximum mass of spherical neutron stars is relatively large $\gtrsim 2.3\ M_\odot$, the collapse would not occur for a rapidly rotating remnant neutron star but for $f_r \lesssim 1.05$. Then the next issue is

whether we can find a self-consistent solution for such collapses, because f_r is determined by the angular momentum dissipation process in the postmerger stage. In the following, we show several realistic scenarios for this process in some of equations of state that we select.

B. Method

For each equation of state, we try to find a solution that satisfies the conservation relations of energy and angular momentum self-consistently. We will have a brief summary of our model by analyzing the degree of freedoms (d.o.f.) of all unknown variables here. There are in total 14 variables in the conservation law of rest mass, energy, and angular momentum [cf. Eq. (2.1), (2.2), and (2.11)]. Nevertheless, M is determined by observation and M_* is related to M by factor f_0 which could be determined once a model equation of state is assumed. Similarly, according to the marginally stable solution results, M_f and J_f are fixed once M_{*f} is fixed and an equation of state is given. Hence, there is only one d.o.f. among M_f, M_{*f}, and J_f. J_0 is given by Eq. (3.1). There are 8 other variables left: E_ν and J_ν are related by Eq. (2.13), $E_{GW,p}$ and $J_{GW,p}$ are related by Eq. (2.12), $M_{eje} + M_{out}$ and $J_{eje} + J_{out}$ are related by Eq. (2.15) and (2.14). As a consequence, there are only 3 d.o.f. in the remaining 8 variables. In total, there are 4 d.o.f. and we have 3 equations (laws of conservation). Once we have input one parameter, such as $M_{eje} + M_{out}$, and a model equation of state is given, all the other quantities related to the properties of the star at the moment of collapse, the total energy of neutrino emission, and gravitational wave in the postmerger phase could be solved (cf. Table. III). With this analysis we can tell whether the assumed equation of state model is consistent with the observation; for instance, the obtained values of E_ν and $E_{GW,p}$ have to be positive and within a plausible range.

TABLE III. Predicted states of rigidly rotating neutron stars at the onset of collapse for the GW170817 event with several equations of state. The given values of $M_{out} + M_{eje}$ are 0.048 $M_\odot$ (upper), 0.096 $M_\odot$ (middle), and 0.150 $M_\odot$ (lower), respectively. M_f and J_f are shown in units of $M_\odot$ and 10^{49} erg s, respectively. The units of $E_{GW,p}$ and E_ν are $M_\odot c^2$. "..." means that no solution of f_r and f_0/f_{MS} exists for the corresponding equations of state. Associated with the uncertainties in J_0 and $E_{GW,i}$ by $\pm 0.1 \times 10^{49}$ erg s, and 0.005 $M_\odot c^2$, respectively, an uncertainty, typically, of ± 0.007 $M_\odot c^2$ and ∓ 0.012 $M_\odot c^2$, exists in $E_{GW,p}$ and E_ν, respectively. * shows that only solutions with negative values of E_ν are obtained. For EOS-12, no solution for f_r and f_0/f_{MS} exists for $M_{out} + M_{eje} \gtrsim 0.058$ $M_\odot$ and no solution with the positive value of E_ν exists for $M_{out} + M_{eje} \leq 0.15$ $M_\odot$, so that we do not describe the results.

Model	f_0/f_{MS}	f_r	M_f	J_f	$E_{GW,p}$	E_ν
EOS-1	...	...	...	...	...	...
EOS-2	...	...	...	...	...	...
EOS-3	0.935	1.194	2.52	3.89	0.076	0.053
EOS-4	0.931	1.169	2.51	3.71	0.091	0.049
EOS-5	0.936	1.160	2.52	3.59	0.082	0.047
EOS-6	0.930	1.134	2.51	3.35	0.102	0.043
EOS-7	0.926	1.111	2.50	3.11	0.118	0.038
EOS-8	0.921	1.103	2.48	3.01	0.130	0.037
EOS-9	0.922	1.077	2.49	2.65	0.130	0.037
EOS-10	0.923	1.069	2.49	2.51	0.130	0.034
EOS-11	0.910	1.042	2.45	1.98	0.194	0.004
EOS-1	0.939	1.201	2.49	3.84	0.034	0.078
EOS-2	...	...	...	...	...	...
EOS-3	0.935	1.174	2.48	3.62	0.051	0.072
EOS-4	0.930	1.150	2.47	3.43	0.067	0.068
EOS-5	0.935	1.140	2.48	3.30	0.064	0.059
EOS-6	0.929	1.114	2.46	3.04	0.083	0.057
EOS-7	0.924	1.092	2.45	2.78	0.100	0.051
EOS-8	0.920	1.084	2.44	2.67	0.112	0.051
EOS-9	0.920	1.058	2.44	2.26	0.118	0.045
EOS-10	0.921	1.050	2.44	2.09	0.120	0.040
EOS-11	0.908	1.023	2.41	1.44	0.188	0.006
EOS-1	0.938	1.178	2.44	3.54	0.008	0.098
EOS-2	0.940	1.162	2.45	3.39	0.024	0.079
EOS-3	0.934	1.151	2.43	3.31	0.025	0.092
EOS-4	0.929	1.127	2.42	3.10	0.041	0.088
EOS-5	0.935	1.118	2.43	2.96	0.046	0.071
EOS-6	0.928	1.092	2.42	2.68	0.064	0.070
EOS-7	0.923	1.070	2.40	2.38	0.083	0.063
EOS-8	0.918	1.062	2.39	2.25	0.094	0.064
EOS-9	0.918	1.037	2.39	1.75	0.109	0.051
EOS-10	0.920	1.028	2.39	1.54	0.114	0.043
EOS-11*	...	...	...	...	...	...

In this analysis, we employ M_f, R_{MS} (circumferential radius), and Ω_{MS} (angular velocity) for rigidly rotating neutron stars at turning points as M_{MNS}, R_{MNS}, and Ω_{MNS}, respectively. f_{MS} is also found from a solution of rigidly rotating neutron stars at turning points. f_0 is calculated from the solutions of spherical neutron stars of mass 1.35–1.40 $M_\odot$ or 1.20–1.55 $M_\odot$. $E_{GW,i}$ is set to be (0.040 ± 0.005) $M_\odot c^2$. J_0 is determined by Eq. (3.1) for a given value of $R_{1.35}$ and η. Here, the variation in η by ± 0.003 systematically changes the values of $E_{GW,p}$ and E_ν only by at most ± 0.007 $M_\odot$ and ∓ 0.007 $M_\odot$. Hence, we only show the results with $\eta = 0.247$. Since the dependence of $J_{out} + J_{eje}$ on R_{out} is not very strong (compared

with the dependence on $M_{out} + M_{eje}$), we fix R_{out} to be 140 km. On the other hand, $M_{out} + M_{eje}$ has a strong effect on the solution. Thus, we vary it in a wide range (e.g., see Fig. 4).

With these preparations, Eq. (2.17) can be considered as a relation between f_r and f_{MS}. Here, in Eq. (2.17), M is given (2.74 $M_\odot$), f_0 is determined for a given equation of state and each mass of binary, and $M_{out} + M_{eje}$ is an input parameter. An equilibrium sequence of rigidly rotating neutron stars along the turning points for a given equation of state also gives another monotonic relation between these two variables as found in Fig. 2. Thus, we first determine f_r and f_{MS} by solving a simultaneous equation composed of two independent relations and specify a
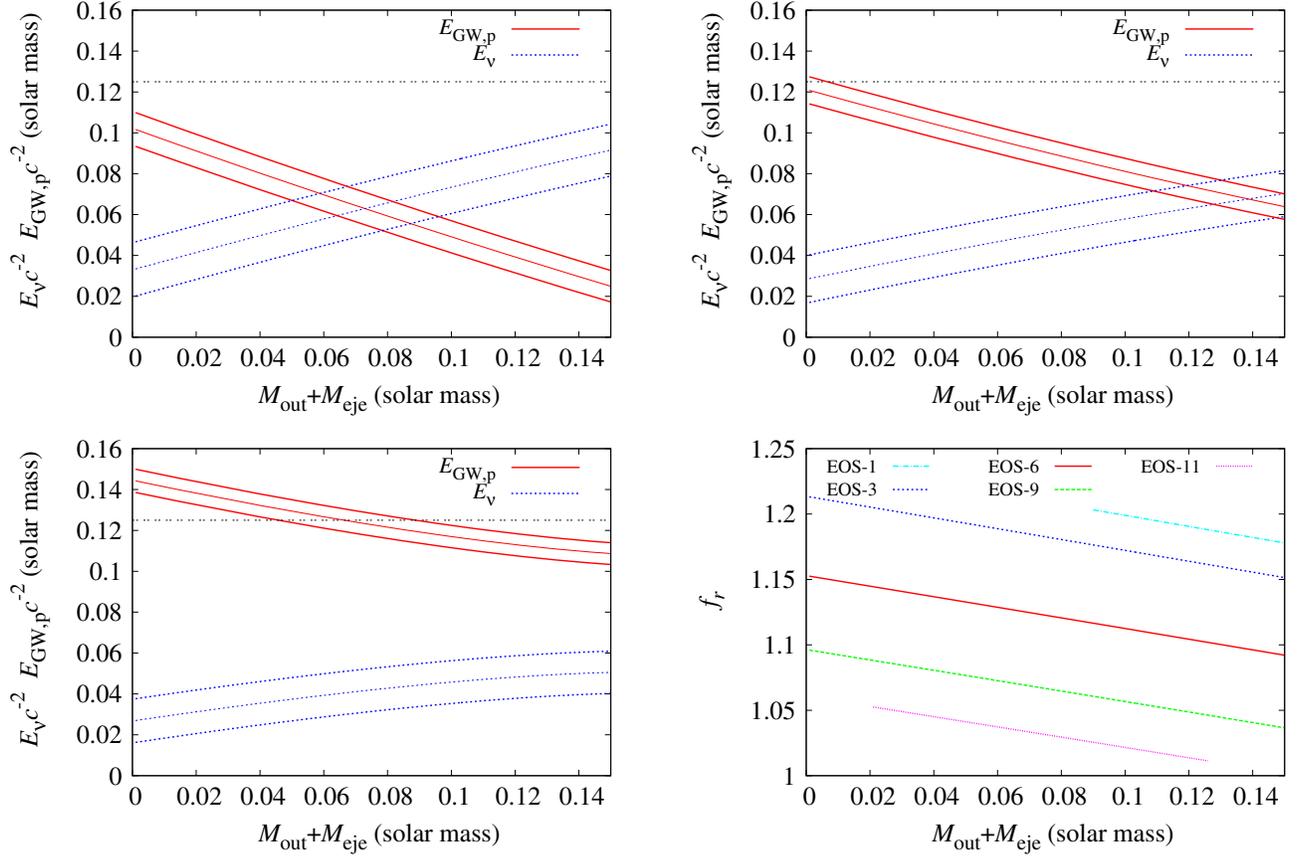
FIG. 4.   Top-left, top-right, and bottom-left panels display $E_{\mathrm{GW,p}}$ and E_ν as functions of $M_{\mathrm{out}} + M_{\mathrm{eje}}$ for EOS-3, 6, and 9, respectively, and for the 1.35–1.40 $M_\odot$ case. Associated with the uncertainties in J_0 and $E_{\mathrm{GW,i}}$, an uncertainty exists in $E_{\mathrm{GW,p}}$ and E_ν. The three curves for each plot in the top-left, top-right, and bottom-left panels denote the upper and lower bounds (thick curves) as well as the central value (thin curve) for $E_{\mathrm{GW,p}}$ and E_ν. The horizontal dot-dot line shows $E_{\mathrm{GW,p}} = 0.125\ M_\odot c^2$ (plausible upper limit of $E_{\mathrm{GW,p}}$ [22]). Bottom-right panel shows f_r as a function of $M_{\mathrm{out}} + M_{\mathrm{eje}}$ for EOS-1, 3, 6, 9, and 11. For EOS-1, the solution for f_r does not exist for small value of $M_{\mathrm{out}} + M_{\mathrm{eje}}$. For EOS-11, E_ν becomes negative for $M_{\mathrm{out}} + M_{\mathrm{eje}} \leq 0.02\ M_\odot$ and $\geq 0.127\ M_\odot$, and, thus, we do not plot the solution for these ranges.

model for the rigidly rotating neutron star at a turning point. (We note that for some equations of state, e.g., EOS-12, the solution does not exist.) We can then obtain J_f, M_f, Ω_{MS}, and R_{MS} for this model using the monotonic relations of $f_{\mathrm{MS}}(J_f)$, $M_f(J_f)$, $\Omega_{\mathrm{MS}}(J_f)$, and $R_{\mathrm{MS}}(J_f)$: cf. Fig. 2.

We can subsequently determine $E_{\mathrm{GW,p}} + E_\nu$ and $J_{\mathrm{GW,p}} + J_\nu$ from Eqs. (2.8) and (2.11). For Eq. (2.11), we employ J_0, $M_{\mathrm{MNS}}(=M_f)$, R_{out}, $R_{\mathrm{MNS}}(=R_{\mathrm{MS}})$, f, and $\Omega(=\Omega_{\mathrm{MS}})$ for each equation of state. Then these two relations, $E_{\mathrm{GW,p}} + E_\nu = \mathrm{const}$ and $J_{\mathrm{GW,p}} + J_\nu = \mathrm{const}$, constitute a simultaneous equation for $E_{\mathrm{GW,p}}$ and E_ν because we have already given the values of R_{MNS}, Ω, and f, which are necessary to relate $J_{\mathrm{GW,p}}$ and J_ν to $E_{\mathrm{GW,p}}$ and E_ν, respectively. Thus, these two quantities are immediately determined, if the solution exists. (Again we note that for some equations of state, a physical solution does not exist: see below.)

C. Results

Table III shows the solutions that self-consistently satisfy the conservation relations of energy and angular momentum

for each equation of state with the selected values of $M_{\mathrm{out}} + M_{\mathrm{eje}}$; 0.048 $M_\odot$, 0.096 $M_\odot$, and 0.150 $M_\odot$. Figure 4 also shows representative results: The top-left, top-right, and bottom-left panels display $E_{\mathrm{GW,p}}$ and E_ν as functions of $M_{\mathrm{out}} + M_{\mathrm{eje}}$ for EOS-3, 6, and 9, respectively, and the bottom-right panel shows f_r as a function of $M_{\mathrm{out}} + M_{\mathrm{eje}}$ for EOS-1, 3, 6, 9, and 11. Here, associated with the uncertainties in J_0 and $E_{\mathrm{GW,i}}$ by $\pm 0.1 \times 10^{49}$ erg s, and 0.005 $M_\odot c^2$, respectively, an uncertainty, typically, of $\pm 0.007\ M_\odot c^2$ and $\mp 0.012\ M_\odot c^2$, exists in $E_{\mathrm{GW,p}}$ and E_ν, respectively. The three curves for each plot in the top-left, top-right, and bottom-left panels of Fig. 4 denote the upper and lower bounds as well as the central value for $E_{\mathrm{GW,p}}$ and E_ν. In addition, the change of f_0 from the 1.35–1.40 $M_\odot$ case to the 1.20–1.55 $M_\odot$ case varies $E_{\mathrm{GW,p}}$ and E_ν typically by $-0.003\ M_\odot c^2$ for both quantities.

For EOS-12, no solution is found for given parameters. The reason for this is that (i) for large values of $M_{\mathrm{out}} + M_{\mathrm{eje}}$, the predicted final mass of the remnant neutron star, M_f, becomes smaller than M_{max}, and,

hence, no solution with $f_r \geq 1$ is present; and (ii) for $M_{out} + M_{eje} \lesssim 0.057\, M_{\odot}$, the value of f_r is determined but physical (positive) values for the set of $(E_{GW,p}, E_\nu)$ are not found. If this type of equation of state with $M_{max} \gtrsim 2.4\, M_{\odot}$ would be the real one, the final outcome should be a stable neutron star in the GW170817 event. However, this is not likely as we discuss in Sec. III D.

For EOS-1 and 2 for which M_{max} is rather small, $\lesssim 2.1\, M_{\odot}$, we often fail to find a solution. The reason for this is that Eq. (2.17) can be satisfied only for a high value of $f_r \sim 1.2$, and, thus, for small values of $M_{out} + M_{eje} \lesssim 0.09\, M_{\odot}$, any solution cannot be present (cf. Fig. 3 and the bottom-right panel of Fig. 4). However, this fact does not imply that these equations of state with $M_{max} \lesssim 2.1\, M_{\odot}$ cannot be accepted. It is still possible that our assumption described in the first paragraph of Sec. II might be inappropriate (i.e., the collapse of the remnant neutron star to a black hole might occur before a rigidly rotating state was reached). If the equation of state with a low value of M_{max} would be the real one, the collapse to a black hole could occur in a stage that the remnant neutron star is differentially rotating for the GW170817 event. If so, the value of f_r is larger than $\gtrsim 1.2$, and, thus, the collapse would occur within the angular momentum transport timescale of the remnant neutron star.

Table III and Fig. 4 show that for EOS-3–7 for which $M_{max} = 2.10$–$2.25\, M_{\odot}$, we find solutions with plausible values of $E_{GW,p}$ and E_ν as $0.03\, M_{\odot} c^2 \lesssim E_{GW,p} \lesssim 0.11\, M_{\odot} c^2$ and $0.03\, M_{\odot} c^2 \lesssim E_\nu \lesssim 0.10\, M_{\odot} c^2$ for plausible values of $M_{out} + M_{eje}$. Also, as Fig. 4 illustrates for EOS-3 and 6, reasonable solutions exist for a wide range of $M_{out} + M_{eje}$ for this class of the equations of state. Here, the value of E_ν indicates that the predicted lifetime of the remnant neutron star in these equations of state is of order 0.1 s to 1 s, which is also quite reasonable. Thus, we conclude that we do not have any reason to exclude equations of state with $2.10\, M_{\odot} \lesssim M_{max} \lesssim 2.25\, M_{\odot}$. It should be emphasized that for these cases, the value of f_r is not always close to ~ 1.2 but in a wide range between 1.07 and 1.20 (see the bottom-right panel of Fig. 4). Thus, $f_r \approx 1.2$ does not always hold for many candidate equations of state.

For EOS-9 and 10, for which $M_{max} \approx 2.30\, M_{\odot}$–$2.33\, M_{\odot}$, we can also find solutions. However, for these cases, a highly efficient energy dissipation by gravitational radiation with $E_{GW,p} \gtrsim 0.11\, M_{\odot}$ is necessary in particular for small values of $M_{out} + M_{eje}$ (see the bottom-left panel of Fig. 4). As found from Table II, the maximum rotational kinetic energy of the rigidly rotating neutron stars is $T_{MS,R} \approx 2.5 \times 10^{53}$ erg $\approx 0.125\, M_{\odot} c^2$. This implies that the energy dissipated by gravitational radiation has to be comparable to the rotational kinetic energy of the remnant neutron star. To know if this class of equations of state is really viable, we have to perform a numerical-relativity

simulation to check whether such efficient gravitational radiation is possible or not. However, this is beyond the scope of this paper and is left for our future study. The bottom-right panel of Fig. 4 illustrates that for this class of equations of state, the value of f_r has to be small (≤ 1.1). That is, an efficient angular momentum dissipation is supposed.

For EOS-8 of $M_{max} \approx 2.25\, M_{\odot}$, we also find solutions with high values of $E_{GW,p}$. However, for this case, with high values of $M_{out} + M_{eje}$, the required value of $E_{GW,p}$ can be reduced. Also, the maximum rotational kinetic energy of the rigidly rotating neutron stars for this equation of state is relatively high, $T_{MS,R} \approx 2.8 \times 10^{53}$ erg $\approx 0.14\, M_{\odot} c^2$. Thus, the restriction for this equation of state is not as strong as for EOS-9 and 10.

For EOS-11, for which $M_{max} \approx 2.35\, M_{\odot}$, the required energy dissipated by gravitational radiation, $E_{GW,p}$, far exceeds $0.125\, M_{\odot} c^2$ that is a plausible maximum value [22]. Moreover, for this case, the $E_{GW,p}$ required exceeds the maximum rotational kinetic energy of the rigidly rotating neutron stars, $T_{MS,R}$. The reason why the required value of $E_{GW,p}$ is very large is that for this case the value of f_r is quite small, ≤ 1.05, and, thus, a large fraction of the angular momentum dissipation, $\sim 4 \times 10^{49}$ erg s, is necessary to reach a marginally stable state. However, for such significant angular momentum dissipation, unrealistically large dissipation by gravitational radiation is necessary. Therefore it is reasonable to exclude these equations of state.

To conclude, it is easy to find model equations of state with $M_{max} \leq 2.25\, M_{\odot}$ that satisfy the conservation laws of energy and angular momentum self-consistently. Also it is not impossible to find model equations of state with $M_{max} \lesssim 2.3\, M_{\odot}$ that satisfy the required laws. For these cases, f_r is not always ≈ 1.2. By contrast, it would not be easy to find an equation of state with $M_{max} \geq 2.35\, M_{\odot}$ that satisfies the required laws.

D. Stable neutron star formation: Not likely

For $M_{max} \gtrsim 2.4\, M_{\odot}$, a stable neutron star could be the final outcome (e.g., EOS-12) as already mentioned above. For this case to be viable, its angular momentum (and rotational kinetic energy) has to be sufficiently small, since the observational results for the electromagnetic counterparts of GW170817 do not show the evidence for the energy injection to ejecta from strong electromagnetic radiation like the magnetic dipole radiation associated with the rotational kinetic energy of the remnant neutron star [9]. If we require that the resulting rotational kinetic energy of the stable neutron star at its age of ~ 100 s is smaller than 10^{52} erg (i.e., by one order of magnitude smaller than the rest-mass energy of ejecta of mass $\sim 0.05\, M_{\odot}$), we need $J_f < 0.5 \times 10^{49}$ erg s (see Fig. 2). Because $J_0 \approx 6.0 \times 10^{49}$ erg s for stiff equations of state like EOS-12, we obtain a constraint as
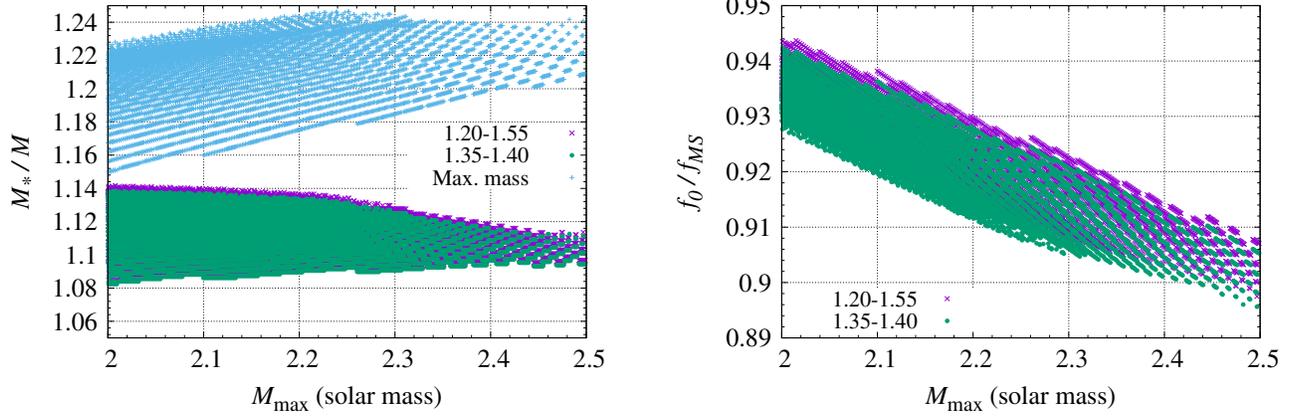
FIG. 5. Left panel: f_0 for the case of 1.20–1.55 $M_\odot$ and 1.35–1.40 $M_\odot$ binary neutron stars and f_{MS} for spherical maximum-mass stars as a function of the maximum mass for a variety of equations of state. Right panel: The same as the left panel but for f_0/f_{MS}. We plot the data with equations of state by which 2 $M_\odot$ neutron stars are reproduced and dimensionless tidal deformability of 1.35 $M_\odot$ star, $\Lambda_{1.35}$, is smaller than 1000.

$$J_{GW,p} + J_\nu + J_{out} + J_{eje} \gtrsim 5.5 \times 10^{49} \text{ erg s} \approx 0.9 J_0. \quad (3.2)$$

Thus, it is necessary for the remnant neutron star to relax to a fairly slow rotation state close to a spherical star.

Figure 5 shows $f_0/f_{MS} \geq 0.90$ ($f_{MS} \sim 1.2$) for spherical neutron stars of $M_{max} \approx 2.4\ M_\odot$. Then we also obtain the following conditions from Eq. (2.8) and $E_{GW,i} = (0.040 \pm 0.005)\ M_\odot$:

$$(E_{GW,p} + E_\nu)c^{-2} + (M_{out} + M_{eje})\left(1 - \frac{1}{f_{MS}}\right)$$
$$\leq (0.234 \pm 0.005)\ M_\odot. \quad (3.3)$$

Here, we supposed that the remnant neutron star would be located along a stable branch near the marginally stable sequence, and hence, we employed the equations derived in Sec. II.

In the hypothesis of this subsection, the remnant is long-lived and it is natural to suppose that $E_\nu \sim 0.1\ M_\odot c^2 \approx 2 \times 10^{53}$ erg or more [21]. Note that it is often mentioned that the total energy dissipated by the neutrino emission from a protoneutron star formed in each supernova would be $\sim(2-3) \times 10^{53}$ erg (e.g., Ref. [36]). Here, the value is larger for a larger mass of the protoneutron stars. The remnant neutron star of binary neutron star mergers is more massive and hotter than the protoneutron star, and hence, it is natural to consider $E_\nu \gtrsim 3 \times 10^{53}$ erg. In the following, we conservatively assume that $E_\nu = 3 \times 10^{53}$ erg $\approx 0.15\ M_\odot c^2$. For this case, we can estimate as $J_\nu \sim 0.5 \times 10^{49}$ erg s using Eq. (2.13).

We also suppose $M_{out} \ll M_{eje}$ for $\tau \gtrsim 100$ s in the following because the torus matter would accrete onto the neutron star or be ejected from the system by viscous angular momentum transport and/or propeller effect [37].

Equation (3.3) with $M_{out} = 0$ gives a constraint as $(E_{GW,p} + E_\nu)c^{-2} + M_{eje}(1 - 1/f_{MS}) \leq 0.24\ M_\odot$. For $E_\nu = 0.15\ M_\odot c^2$, we obtain

$$E_{GW,p} c^{-2} + M_{eje}\left(1 - \frac{1}{f_{MS}}\right) \leq 0.09\ M_\odot. \quad (3.4)$$

Now we consider two extreme cases (assume $f_{MS} = 1.2$): $E_{GW,p} = 0.085\ M_\odot c^2$ and $M_{eje} = 0.03\ M_\odot$ (minimum ejecta mass required for the GW170817 event), and $E_{GW,p} = 0.055M$ and $M_{eje} = 0.15\ M_\odot$. Here, for the GW170817 event, the value of M_{eje} would be smaller than 0.15 $M_\odot$.

For $E_{GW,p} = 0.085\ M_\odot c^2$ and $f = 2.5$ kHz (which would be the possible lowest value), $J_{GW,p} \approx 1.9 \times 10^{49}$ erg s. For $M_{eje} = 0.03\ M_\odot$, the ejection of the angular momentum would be $\approx 0.5 \times 10^{49}$ erg s for $R_{eje} \approx 200$ km [cf. Eq. (2.15)]. Since $J_\nu \approx 0.5 \times 10^{49}$ erg s, the constraint of Eq. (3.2) cannot be satisfied in this model at all.

For $M_{eje} = 0.15\ M_\odot$, the ejection of the angular momentum would be $\approx 2.5 \times 10^{49}$ erg s for $R_{eje} \approx 200$ km [e.g., Eq. (2.15)]. With $E_{GW,p} = 0.055\ M_\odot c^2$ and $f = 2.5$ Hz, $J_{GW,p} \approx 1.3 \times 10^{49}$ erg s. For $J_\nu \approx 0.5 \times 10^{49}$ erg s, it is found that the constraint of Eq. (3.2) cannot be also satisfied in this model.

As found from the above analysis, for a larger value of M_{eje}, $J_{GW,p} + J_\nu + J_{eje}$ increases. However, for the GW170817 event, M_{eje} is not very likely to be larger than 0.15 $M_\odot$. If f is smaller than 2.5 kHz, $J_{GW,p}$ would be larger. However, a number of numerical-relativity simulations have shown $f \geq 2$ kHz [28,29,38]; $J_{GW,p}$ could be increased only by 20%. Thus, we conclude that it is quite difficult to find a mechanism of the angular momentum dissipation by $\approx 0.9 J_0$ in a short timescale of ~ 100 s.

Since the values of E_ν, R_{eje}, M_{eje}, and f have uncertainty, it is not possible to fully exclude the possibility of forming a stable neutron star. In particular, in case that E_ν could be much smaller than 3×10^{53} erg, the angular momentum of the remnant neutron star could be smaller than $0.1 J_0$, e.g., by setting $E_{GW,p} = 0.125 \, M_\odot c^2$, $E_\nu = 0.09 \, M_\odot c^2$, and $M_{eje} = 0.15 \, M_\odot$, with $f = 2.5$ kHz and $R_{eje} = 200$ km. However, we need a (unphysical) fine tuning, and hence, such a possibility would not be very likely.

IV. SUMMARY

We study the constraint on the maximum mass of cold spherical neutron stars coming from the observational results of GW170817 more strictly than our previous study. We develop a framework which employs not only energy conservation law but also the angular momentum conservation one, as well as solid results of the latest numerical-relativity simulations and of neutron stars in equilibrium.

In this framework, we postulate that a massive neutron star was formed as a remnant after the merger in the GW170817 event, and the collapse occurred after the remnant neutron star relaxed to a rigidly rotating state. Thus, we construct several rigidly rotating neutron stars in equilibrium as models of the remnant neutron stars at the onset of collapse. In the analysis, we first give plausible values for $M_{out} + M_{eje}$, taking into account the observational results of electromagnetic counterparts of GW170817. Then, the energy conservation law gives a relation between the maximum mass, M_{max}, and angular momentum of the remnant neutron star at the onset of collapse. This relation indicates that for smaller values of M_{max}, the collapse occurs at higher angular momentum (i.e., at larger values of f_r: cf. Fig. 3). We also find the correlation between M_{max} and M_f: the gravitational mass at the onset of collapse. Thus, for smaller values of M_{max}, M_f has to be larger; i.e., less energy and angular momentum have to be dissipated prior to the onset of collapse.

We find that the energy conservation laws can be satisfied for a wide range of equations of state with various values of $f_r = 1.0$–1.2. Also, it is found that the combination of energy and angular momentum conservation laws gives plausible values of $E_{GW,p}$ and E_ν for the equations of state in which M_{max} is between $\sim 2.1 \, M_\odot$ and $\sim 2.3 \, M_\odot$. In particular, the cases of $M_{max} \lesssim 2.25 \, M_\odot$ result in quite plausible values of $E_{GW,p}$ and E_ν. For $M_{max} = 2.30 \, M_\odot$–$2.35 \, M_\odot$, it is still possible to find solutions although for such a case, we need to require large energy dissipation by gravitational radiation, $E_{GW,p} \gtrsim 0.11 \, M_\odot c^2$. It is also found that if the value of M_{max} is not very high, i.e., $M_{max} \leq 2.1 \, M_\odot$, the collapse is likely to occur before the velocity profile of the remnant neutron star relaxes to a rigidly rotating state. Thus, we infer that if $M_{max} \lesssim 2.1 \, M_\odot$, the remnant neutron star collapses to a black hole in the timescale of angular momentum transport inside it.

The previous analysis often assumes $f_r \approx 1.2$ [7–10], i.e., the collapse occurs at a rapidly rotating stage of the remnant neutron star. As Fig. 3 shows, this assumption together with the energy conservation law would automatically lead to an inaccurate conclusion that the value of M_{max} is small, $\lesssim 2.1 \, M_\odot$ (i.e., the conclusion is derived from the assumption). The lesson obtained from our present analysis is that inappropriate assumptions could lead to an inaccurate constraint on the maximum mass.

The framework of our analysis for the maximum mass of neutron stars developed in this paper will be applied for future events, in which the remnant after the mergers is a massive neutron star that eventually collapses to a black hole, by simply replacing the values of M and $M_{out} + M_{eje}$. This analysis will be in particular interesting if postmerger gravitational waves are observed in the future. For this case, $E_{GW,p}$ and $J_{GW,p}$ will be constrained, and, then, the constraint for the equation of state and the value of M_{max} will be better imposed. Furthermore, it will be also feasible to infer how much energy is carried away by neutrinos.

APPENDIX: MODEL EQUATIONS OF STATE

To model the neutron-star equation of state with a small number of parameters, we employ a piecewise polytrope introduced by Read et al. [39]. It is a phenomenologically parametrized equation of state of the form:

$$P(\rho) = \kappa_i \rho^{\Gamma_i} \quad \text{for } \rho_{i-1} \leq \rho < \rho_i \quad (1 \leq i \leq n), \quad \text{(A1)}$$

where n is the number of the pieces used to parametrize an equation of state, ρ_i is the rest-mass density at the boundary of two neighboring ith and $(i+1)$th pieces, κ_i is the polytropic constant for the ith piece, and Γ_i is the adiabatic index for the ith piece. Here, $\rho_0 = 0$, and other parameters $(\rho_i, \kappa_i, \Gamma_i)$ are freely chosen. Requiring the continuity of the pressure at each value of ρ_i, $2n$ free parameters, (κ_i, Γ_i), determines the equation of state completely. The specific internal energy, ε, is determined by the first law of thermodynamics and continuity of each variable at ρ_i.

In this paper, we employ the case of $n = 3$ and fix $\rho_2 = 10^{15}$ g/cm³ (and $\rho_3 = \infty$). The lowest-density piece

models the crust equation of state, and the other two do the core equation of state. Following Ref. [39], the equation of state for the crust region is fixed by $\Gamma_1 = 1.35692395$ and $\kappa_1/c^2 = 3.99873692 \times 10^{-8}$ $(\text{g/cm}^3)^{1-\Gamma_1}$. The equation of state for the core region is determined by two adiabatic indices, Γ_2 and Γ_3, and the pressure, p, at a fiducial density $\rho_f = 10^{14.7}$ g/cm^3. Here, p is closely related to the radius and tidal deformability of neutron stars [40]. For Γ_2, we employ a wide range of values between 2.10–5.00. Γ_3 is chosen to be small values in a narrow range between 2.00–2.91, because for the large values, the sound speed exceeds the speed of light even for stable neutron stars, while for the small values, the maximum mass for given equations of state cannot exceed $2 M_\odot$ [33]. The value of $\log_{10} p$ is varied between 33.8 and 34.8. Here, for large values of Γ_2, only small values of p are accepted (e.g., for $\Gamma_2 = 4.0$ and 5.0, $p \lesssim 10^{34.35}$ dyn/cm^2 and $p \lesssim 10^{33.9}$ dyn/cm^2, respectively). If this condition is not satisfied, the sound velocity exceeds the speed of light near $\rho \sim 10^{15}$ g/cm^3. With the given values of Γ_2, Γ_3, and p, κ_2, κ_3, and ρ_1 are determined as $\kappa_2 = p\rho_f^{-\Gamma_2}$, $\kappa_3 = \kappa_2 \rho_2^{\Gamma_2 - \Gamma_3}$, and $\rho_1 = (\kappa_1/\kappa_2)^{1/(\Gamma_2 - \Gamma_1)}$.

We analyzed the values of f_0 and f_{MS} for spherical neutron stars with the piecewise polytropes. Figure 5 displays a result. In this figure, we plot the data in the piecewise polytropes with which $2 M_\odot$ neutron stars are reproduced and dimensionless tidal deformability of $1.35 M_\odot$ neutron stars satisfies $\Lambda_{1.35} \le 1000$, taking into account the results of GW170817 [1]. It is found that f_0 and f_{MS} are in a wide range approximately between 1.08 and 1.14 and between 1.14 and 1.24, respectively. Because f_0 and f_{MS} are weakly correlated, f_0/f_{MS} is not distributed as widely as f_{MS}, but it is still in a fairly wide range as 0.895–0.945. This value depends weakly on each mass of binaries: For 1.20–1.55 $M_\odot$ binaries, the values of f_0/f_{MS} are 0.2–0.3% larger than those for 1.35–1.40 $M_\odot$ binaries for a given equation of state.

One interesting and key fact for the context of the present paper is that f_0/f_{MS} is correlated with M_{max}; for larger value of f_0/f_{MS}, the maximum mass of neutron stars is smaller. The reason for this is that for the equations of state with smaller maximum mass, the neutron star at the maximum mass is less compact and thus has a smaller value of f_{MS}. This fact implies that for smaller maximum mass, the mass of the remnant neutron-star mass at the onset of collapse, $M_f = M f_0/f_{MS} - (M_{out} + M_{eje})/f_{MS}$, is larger [see Eq. (2.4)], and hence, the merger remnant is more subject to gravitational collapse. We note that the upper boundary of f_0/f_{MS} for a give value of M_{max} is determined by the condition of $\Lambda_{1.35} \le 1000$.

[1] B. P. Abbott *et al.*, Phys. Rev. Lett. **119**, 116101 (2017).

[2] B. P. Abbott *et al.*, Astrophys. J. **848**, L12 (2017).

[3] B. P. Abbott *et al.*, Phys. Rev. Lett. **121**, 161101 (2018); Phys. Rev. D **9**, 011001 (2019).

[4] S. De, D. Finstad, J. M. Lattimer, D. A. Brown, E. Berger, and C. M. Biwer, Phys. Rev. Lett. **121**, 091102 (2018).

[5] B. P. Abbott *et al.*, Astrophys. J. **848**, L13 (2017).

[6] M. Tanaka *et al.*, Publ. Astron. Soc. Jpn. **69**, 102 (2017); D. Kasen, B. D. Metzger, J. Barnes, E. Quataert, and E. Ramirez-Ruiz, Nature (London) **551**, 80 (2017).

[7] L. Rezzolla, E. R. Most, and L. R. Weih, Astrophys. J. **852**, L25 (2018).

[8] M. Ruiz, S. L. Shapiro, and A. Tsokaros, Phys. Rev. D **97**, 021501 (2018).

[9] B. Margalit and B. D. Metzger, Astrophys. J. **850**, L19 (2017).

[10] M. Shibata, S. Fujibayashi, K. Hotokezaka, K. Kiuchi, K. Kyutoku, Y. Sekiguchi, and M. Tanaka, Phys. Rev. D **96**, 123012 (2017).

[11] A. Perego, D. Radice, and S. Bernuzzi, Astrophys. J. **850**, L37 (2017).

[12] J. Lippuner, R. Fernández, L. Robert, F. Foucart, D. Kasen, B. D. Metzger, and C. D. Ott, Mon. Not. R. Soc. Astron. **472**, 904 (2017).

[13] B. D. Metzger and A. L. Piro, Mon. Not. R. Astron. Soc. **439**, 3916 (2014).

[14] D. J. Price and S. Rosswog, Science **312**, 719 (2006); K. Kiuchi, K. Kyutoku, Y. Sekiguchi, M. Shibata, and T. Wada, Phys. Rev. D **90**, 041502 (2014); K. Kiuchi, P. Cerda-Duran, K. Kyutoku, Y. Sekiguchi, and M. Shibata, Phys. Rev. D **92**, 124034 (2015).

[15] S. Fujibayashi, K. Kiuchi, N. Nishimura, Y. Sekiguchi, and M. Shibata, Astrophys. J **860**, 64 (2018).

[16] J. L. Friedman, J. R. Ipser, and R. Sorkin, Astrophys. J. **325**, 722 (1988).

[17] G. B. Cook, S. L. Shapiro, and S.A Teukolsky, Astrophys. J. **423**, 823 (1994).

[18] C. Alcock, E. Farhi, and A. Olinto, Astrophys. J. **310**, 261 (1986); A. Drago, A. Lavagno, and G. Pagliara, Phys. Rev. D **89**, 043014 (2014); M. G. Alford, S. Han, and M. Prakash, Phys. Rev. D **88**, 083013 (2013); G. Boz- zola, P. L. Espino, C. D. Lewin, and V. Paschalidis, arXiv:1905.00028; E. Zhou, A. Tsokaros, K. Uryū, R. X. Xu, and M. Shibata, arXiv:1902.09361; R. D. Pietri, A. Drago, A. Feo, G. Pagliara, M. Pasquali, S. Traversi, and G. Wiktorow- icz, arXiv:1904.01545.

[19] B. D. Metzger and R. Fernández, Mon. Not. R. Astron. Soc. **441**, 3444 (2014).

[20] A. Perego, S. Rosswog, R. M. Cabezon, O. Korobkin, R. Kappeli, A. Arcones, and M. Liebendorfer, Mon. Not. R. Astron. Soc. **443**, 3134 (2014).

[21] S. Fujibayashi, S. Wanajo, Y. Sekiguchi, K. Kyutoku, N. Nishimura, K. Kiuchi, and M. Shibata (to be published).

[22] F. Zappa, S. Bernuzzi, D. Radice, A. Perego, and T. Dietrich, Phys. Rev. Lett. **120,** 111101 (2018).

[23] M. Shibata and K. Kiuchi, Phys. Rev. D **95,** 123003 (2017).

[24] Y. Sekiguchi, K. Kiuchi, K. Kyutoku, and M. Shibata, Phys. Rev. Lett. **107,** 051102 (2011); Phys. Rev. D **91,** 064059 (2015); Phys. Rev. D **93,** 124046 (2016).

[25] F. Foucart, R. Haas, M. D. Duez, E. O'Connor, C. D. Ott, L. Roberts, L. E. Kidder, J. Lippuner, H. P. Pfeiffer, and M. A. Scheel, Phys. Rev. D **93,** 044019 (2016).

[26] D. Radice, F. Galeazzi, J. Lippuner, L. F. Roberts, C. D. Ott, and L. Rezzolla, Mon. Not. R. Astron. Soc. **460,** 3255 (2016).

[27] C. Breu and L. Rezzolla, Mon. Not. R. Astron. Soc. **459,** 646 (2016).

[28] A. Bauswein, H.-T. Janka, K. Hebeler, and A. Schwenk, Phys. Rev. D **86,** 063001 (2012).

[29] K. Hotokezaka, K. Kiuchi, K. Kyutoku, T. Muranushi, Y. Sekiguchi, M. Shibata, and K. Taniguchi, Phys. Rev. D **88,** 044026 (2013).

[30] K. Kiuchi, K. Kawaguchi, K. Kyutoku, Y. Sekiguchi, and M. Shibata, arXiv:1907.03790.

[31] T. W. Baumgarte and S. L. Shapiro, Astrophys. J. **504,** 431 (1998).

[32] M. Shibata and K. Uryū, Phys. Rev. D **61,** 064001 (2000); M. Shibata, K. Taniguchi, and K. Uryū, Phys. Rev. D **71,** 084021 (2005).

[33] P. Demorest, T. Pennucci, S. Ransom, M. Roberts, and J. Hessels, Nature (London) **467,** 1081 (2010); J. Antoniadis *et al.*, Science **340,** 1233232 (2013); H. T. Cromartie *et al.*, arXiv:1904.06759.

[34] J. D. Kaplan *et al.*, Astrophys. J. **790,** 19 (2014).

[35] S.-Z. Li, L.-D. Liu, Y.-W. Yu, and B. Zhang, Astrophys. J. **861,** L12 (2018).

[36] Y. Suwa *et al.*, arXiv:1904.09996.

[37] A. L. Piro and C. D. Ott, Astrophys. J. **736,** 108 (2011).

[38] K. Takami, L. Rezzolla, and L. Baiotti, Phys. Rev. D **91,** 064001 (2015).

[39] J. Read, B. Lackey, J. L. Friedman, and B. Owen, Phys. Rev. D **79,** 124032 (2009).

[40] J. M. Lattimer and M. Prakash, Astrophys. J. **550,** 426 (2001).